Rapid Communications

Experimental conditions for the observation of electron-hole superfluidity in GaAs heterostructures

Samira Saberi-Pouya,[1] Sara Conti,[1,2] Andrea Perali,[3] Andrew F. Croxall,[4] Alexander R. Hamilton,[5] François M. Peeters,[1] and David Neilson[1,5]

[1]*Department of Physics, University of Antwerp, Groenenborgerlaan 171, 2020 Antwerpen, Belgium*
[2]*Physics Division, School of Science and Technology, Università di Camerino, 62032 Camerino (MC), Italy*
[3]*Supernano Laboratory, School of Pharmacy, Università di Camerino, 62032 Camerino (MC), Italy*
[4]*Cavendish Laboratory, University of Cambridge, J.J. Thomson Avenue, Cambridge CB3 0HE, United Kingdom*
[5]*ARC Centre of Excellence for Future Low Energy Electronics Technologies, School of Physics, The University of New South Wales, Sydney, New South Wales 2052, Australia*

(Received 14 October 2019; revised manuscript received 8 January 2020; accepted 28 February 2020; published 6 April 2020)

The experimental parameter ranges needed to generate superfluidity in optical and drag experiments in GaAs double quantum wells are determined using a formalism that includes self-consistent screening of the Coulomb pairing interaction in the presence of the superfluid. The very different electron and hole masses in GaAs make this a particularly interesting system for superfluidity with exotic superfluid phases predicted in the BCS-Bose-Einstein condensation crossover regime. We find that the density and temperature ranges for superfluidity cover the range for which optical experiments have observed indications of superfluidity but that existing drag experiments lie outside the superfluid range. We also show that, for samples with low mobility with no macroscopically connected superfluidity, if the superfluidity survives in randomly distributed localized pockets, standard quantum capacitance measurements could detect these pockets.

DOI: 10.1103/PhysRevB.101.140501

Although Bose-Einstein condensation (BEC) and the BCS-BEC crossover phenomena in superfluidity have been extensively studied for ultracold Fermi atoms [1–3], it is probable that practical applications will, instead, be based on superfluidity in solid-state devices. Existence of superfluidity in coupled atomically flat layers in semiconductor heterostructures has been theoretically predicted [4,5], whereas recent observations of dramatically enhanced tunneling at equal densities in electron-hole double bilayer sheets of graphene [6,7] and in double monolayers of transition-metal dichalcogenide monolayers [8,9] are strong experimental indications for electron-hole condensation [10].

Electron-hole superfluidity and the BCS-BEC crossover was first proposed for an excitonic system in a conventional semiconductor heterostructure of double quantum wells in GaAs [11]. This was based on extensions of earlier work on exciton condensation [12–15]. To block electron-hole recombination, Refs. [14,15] proposed spatially separating the electrons and holes in a heterostructure consisting of two layers separated by an insulating barrier.

Superfluidity in GaAs quantum wells differs in significant ways from superfluidity in coupled atomically flat layers. The large band gap in GaAs eliminates the multicondensate effects and multiband screening that are important in graphene [16], and the low-lying conduction and valence bands are nearly parabolic and not dependent on gate potentials.

However, it is the widely different electron and hole effective masses that provide the most dramatic contrast of superfluidity in GaAs compared with superfluidity in other solid-state devices. In GaAs, the masses differ by a large factor: We take $m_e^\star = 0.067 m_e$ and $m_h^\star = 0.3 m_e$. Not only does this have significant consequences for the superfluid properties [17], but also for the screening responses of the electrons and holes, which are significantly different from the equal mass case. In ultracold atomic gases, Dy-K Fermi mixtures have been used to explore the physics of mass-imbalanced strongly interacting Fermi-Fermi mixtures [18].

The large mass difference makes double quantum wells in GaAs a solid-state system uniquely suitable for generating and enhancing exotic superfluid phases that span the BCS-BEC crossover [19]. Such phases can also be expected in mass-imbalanced ultracold atomic gas Fermi mixtures [20] but only at currently inaccessible temperatures [21] $T_c \lesssim 50$ nK. The phases include the Fulde-Ferrell-Larkin-Ovchinnikov (FFLO) phase [22] and the Sarma phase with two Fermi surfaces (breached pair phase) [23]. For GaAs, our estimates for transition temperatures to the FFLO phase are readily accessible experimentally $T_c \sim 0.2$–0.5 K. Potentially even more exciting is the possibility of a Larkin-Ovchinnikov supersolid phase when the masses are unequal [24,25].

For these reasons, experimental realization of superfluidity in GaAs quantum wells is of great interest. A major challenge facing experiments is that electron-hole superfluidity in double layer systems is exclusively a low-density phenomenon because strong screening of the long-range Coulomb pairing interactions suppresses superfluidity above an onset density n_0, and this is low [4,16,26,27]. Nevertheless, there are reports suggesting possible experimental signatures of electron-hole superfluid condensation in GaAs double quantum wells. Some signatures are based on optical observations of indirect exciton luminescence [28–31], whereas others are based on transport measurements of Coulomb drag [32,33].

In this Rapid Communication, we map out the parameter space for GaAs double quantum well heterostructures to determine where electron-hole superfluidity is favored. Important parameters are the widths w of the quantum wells, the thickness t_B of the $Al_xGa_{1-x}As$ insulating barrier, the densities in the wells n (assumed equal), and any perpendicular electric fields. The distance between the peaks of the density distributions of the electrons and holes must be calculated and is usually not simply the distance between the centers of the quantum wells. By establishing the parameter ranges expected for superfluidity, we are able to provide independent corroborative support for the reported experimental signatures suggesting superfluidity.

Existing optical experiments generally use samples with quantum wells and barriers which are narrower than in samples for transport measurements. A major reason is that a problem arises for transport with the narrower wells from interface roughness scattering caused by Al atoms in the insulating barrier diffusing into the well regions. Interface roughness scattering dramatically reduces the mobility, which is an essential consideration for transport measurements. Also, in optical measurements, electron-hole pairs are optically excited in a quantum well and then spatially separated across the barrier by means of a perpendicular electric field. Thus, barriers are generally thinner than those for transport experiments, so the coupling of the electron-hole pairs tends to be stronger for optical measurements.

For the optical experiments, we consider the samples from Refs. [28–30] with 8-nm GaAs quantum wells separated by a 4-nm barrier of $Al_xGa_{1-x}As$ and Ref. [31] with 12-nm wells and a 1.1-nm AlAs barrier. Techniques to optically identify macroscopic spatial coherence were as follows: The appearance in photoluminescence measurements of bright localized spots with enhanced luminescence at fixed points on the sample [28]; the abrupt appearance of a sharp inter-well exciton line in the photoluminescence spectra [31]; an abrupt increase in the amplitude of interference fringes using a Mach-Zehnder interferometer [29] indicating a strong enhancement of the exciton coherence length; quenching of photoluminescence emission as a manifestation of optically dark exciton condensation [30]. Indications of coherent condensation were observed at temperatures of a few kelvins at carrier densities of a few 10^{10} cm^{-2}.

From the samples used in the Coulomb drag experiments [32,33], we examine the narrowest 15-nm wells with the thinnest 10-nm $Al_{0.9}Ga_{0.1}As$ barrier (see Fig. 1). References [32,33] observed a jump in the drag transresistivity around temperatures of $T \sim 0.2$–1 K. A sudden jump can be a signature of a superfluid transition [34], but the observed deviations were not monotonic, sometimes even changing sign, so any signature of condensation was ambiguous.

We start with the Hamiltonian,

$$\mathcal{H} = \sum_{\ell \mathbf{k}} \xi^{\ell}_{\mathbf{k}} c^{\ell\dagger}_{\mathbf{k}} c^{\ell}_{\mathbf{k}} + \frac{1}{2} \sum_{\substack{\ell \neq \ell', \\ \mathbf{q},\mathbf{k},\mathbf{k}'}} V^{\ell\ell'}_{\mathbf{k}-\mathbf{k}'} c^{\ell\dagger}_{\mathbf{k}+(\mathbf{q}/2)} c^{\ell'\dagger}_{-\mathbf{k}+(\mathbf{q}/2)} \times c^{\ell}_{-\mathbf{k}'+(\mathbf{q}/2)} c^{\ell'}_{\mathbf{k}'+(\mathbf{q}/2)}, \quad (1)$$

where $c^{\ell\dagger}_{\mathbf{k}}$ and $c^{\ell}_{\mathbf{k}}$ are creation and destruction operators with label $\ell = e$ (h) for electrons (holes) in their respective quantum wells and $\xi^{\ell}_{\mathbf{k}} = k^2/(2m^{\star}_{\ell}) - \mu^{\ell}$ are the single-particle energy-band dispersion with chemical potentials μ^{ℓ}. Although spin-orbit interactions [37] are, in general, important for the hole bands in GaAs, here, they can be neglected because narrow wells suppress Rashba and Dresselhaus interactions due to the large light-hole heavy-hole splitting. Furthermore, the electric fields across the well here are small, and the hole densities of interest here are low. The $V^{\ell\ell'}_{\mathbf{k}-\mathbf{k}'}$'s are the bare Coulomb interaction potentials between electrons and holes confined in their finite width wells ℓ and ℓ'. The full expressions for $V^{\ell\ell'}_{\mathbf{k}-\mathbf{k}'}$ are found in Sec. S1 of the Supplemental Material [38], which includes Refs. [39–44].

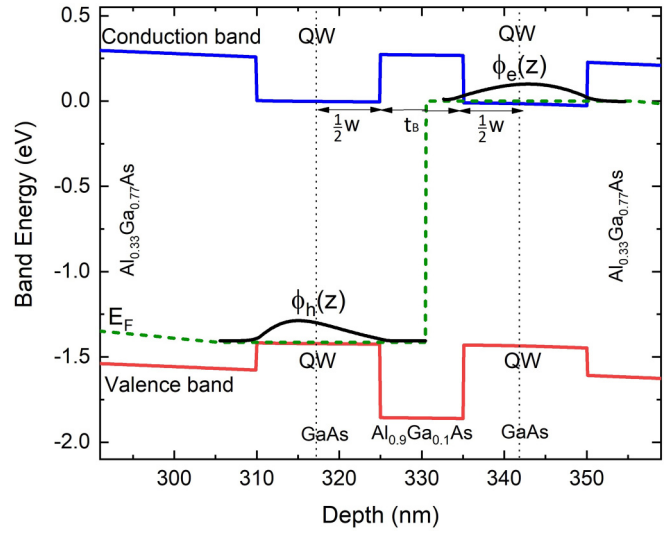

FIG. 1. Conduction and valence bands for a sample from Ref. [32] in the presence of gate potentials and a bias between the wells [35] as obtained using a self-consistent Poisson-Schrödinger solver [36]: quantum well widths: $w = 15$ nm and $Al_{0.9}Ga_{0.1}As$ barrier thickness: $t_B = 10$ nm. The dashed green line: Fermi-level E_F. The vertical black dotted lines mark the centers of the wells. $\phi_e(z)$ and $\phi_h(z)$ are the resulting electron and hole single-particle wave functions confined in the wells. Note that the separation of the peaks in $\phi_e(z)$ and $\phi_h(z)$ is larger than the distance between the centers of the two wells.

The mean-field equations at zero temperature for the superfluid gap $\Delta_{\mathbf{k}}$ and the average chemical potential $\mu = (\mu^e + \mu^h)/2$ for equal electron and hole densities n are as follows:

$$\Delta_{\mathbf{k}} = -\frac{1}{A} \sum_{\mathbf{k}'} V^{sc}_{\mathbf{k}-\mathbf{k}'} \frac{\Delta_{\mathbf{k}'}}{2E_{\mathbf{k}'}}, \quad (2)$$

$$n = \frac{2}{A} \sum_{\mathbf{k}} (v_{\mathbf{k}})^2, \quad (3)$$

where A is the sample surface area, $E_{\mathbf{k}} = \sqrt{\xi^2_{\mathbf{k}} + \Delta^2_{\mathbf{k}}}$ with $\xi_{\mathbf{k}} = \frac{1}{2}(\xi^{\mathrm{e}}_{\mathbf{k}} + \xi^{\mathrm{h}}_{\mathbf{k}})$, and the Bogoliubov coherence factors are as follows:

$$u^2_{\mathbf{k}} = \frac{1}{2}\left(1 + \frac{\xi_{\mathbf{k}}}{E_{\mathbf{k}}}\right); \quad v^2_{\mathbf{k}} = \frac{1}{2}\left(1 - \frac{\xi_{\mathbf{k}}}{E_{\mathbf{k}}}\right). \quad (4)$$

$V^{sc}_{\mathbf{q}}$ is the static screened electron-hole Coulomb interaction in the superfluid state for momentum transfer $\mathbf{q}$, evaluated within the random-phase approximation (RPA) for electrons and

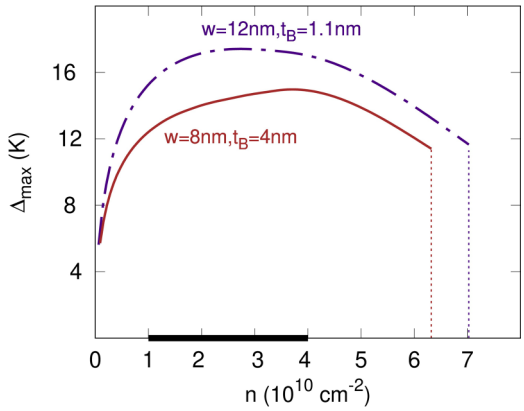

FIG. 2. $\Delta_{\max}$ is the maximum value of the zero-T momentum-dependent superfluid gap as a function of n, the equal electron, and hole densities. The solid red line: $w = 8$ and $t_B = 4$ nm (sample: Refs. [28–30]); dashed-dotted purple line: $w = 12$ and $t_B = 1.1$ nm (sample: Ref. [31]). The horizontal black bar indicates the density range over which anomalous behavior was observed in Refs. [28–30].

holes of unequal masses. The superfluid energy gap Δ near the Fermi surface blocks excitations from the Fermi sea with energies less than Δ. This weakens the effect of screening since low-lying excitations are those needed to screen the long-range Coulomb interactions. The small-$\mathbf{q}$ suppression of screening leads to strong electron-hole pairing peaked at small $\mathbf{q}$, and this can lead to large superfluid gaps. The expressions for $V_{\mathbf{q}}^{sc}$ are given in Sec. S2 of the Supplemental Material [38].

A comparison of the good agreement of zero-T superfluid properties for a double layer electron-hole system calculated using the present mean-field RPA approach [26] with the corresponding results calculated using diffusion quantum Monte Carlo (DQMC) [27] indicates that the present RPA approach should be a quantitatively good approximation.

For a quasi-two-dimensional system, the superfluid transition is a topological transition associated with the Berezinskii-Kosterlitz-Thouless (BKT) transition temperature [45] which depends only on the superfluid stiffness $\rho_s(T)$ [46]: $T^{BKT} = (\pi/2)\rho_s(T^{BKT})$. Provided $T^{BKT} \ll \Delta$ $(T = 0)$, which is the case here, $T^{BKT} \simeq n\{\pi\hbar^2/[8(m_e^\star + m_h^\star)]\}$.

Figure 2 shows $\Delta_{\max}$, the maximum of the zero-T momentum-dependent gap $\Delta_{\mathbf{k}}$ determined from Eq. (2). n is the equal electron and hole density for the GaAs heterostructure samples that were used for the optical observations [28–31]. Robust electron-hole superfluidity is a low-density phenomenon: At higher densities, strong screening greatly weakens the electron-hole coupling, leading to $\Delta_{\max}$ of, at most, a few millikelvins [4,47]. These effects are nicely illustrated in Fig. 2 of Ref. [47]. Superfluidity survives up to the highest densities because there always remains a small residual screened electron-hole pairing interaction. In two dimensions, an arbitrarily weak attractive interaction is known to lead to, at least, one bound state, and in BCS, any bound state generates condensation into a BCS coherent state. Since around n_0, the superfluid order parameter remains finite and retains its symmetry, this is a crossoverlike evolution of the superfluid order parameter as a function of density, and there is no quantum phase transition at zero temperature. The sharp drop seen in $\Delta_{\max}$ near n_0 is, in fact, an artifact of the BCS-RPA mean-field approximation. We know this from a full DQMC calculation in a similar system, which found that the BCS-RPA approximation accurately predicted n_0, but that the decrease in $\Delta_{\max}$ near n_0 is not so abrupt [27].

For densities above the superfluid onset density, the exponentially small order parameter would be destroyed by disorder in a real system. In Fig. 2, we see that near the onset density, $\Delta_{\max}$ increases rapidly to energies $\gtrsim$10 K. This is a self-consistent effect since large superfluid gaps weaken the screening. The widths of the quantum wells and barriers in the experimental samples of Refs. [28–31] are narrow, making the electron-hole pairing interactions relatively strong. This results in high superfluid onset densities, $n_0 \sim 6$ to 7×10^{10} cm^{-2}. The range of densities for which anomalous behavior was observed in Refs. [28–30], indicated by the black bar in Fig. 2, lies within the density range for which we predict superfluidity. This adds independent credence that the observed anomalous behavior is, indeed, associated with superfluidity. We find maximum BKT transition temperatures of a few kelvins.

In Sec. S3 of the Supplemental Material [38] which includes Refs. [48–50], we discuss the property that the superfluidity in the GaAs system is nearly always confined within the crossover regime that separates the BCS regime from the BEC regime. This is due to the strong screening that kills superfluidity in the weakly interacting BCS regime and to the large electron-hole mass difference in GaAs that impedes the system from entering the strongly interacting BEC regime at low densities.

As we have discussed, to get high enough mobilities to avoid localization and allow transport studies, the wells and the barriers need to be wider for the transport drag measurements [32,33] compared with the samples for the optical measurements. We see, in Fig. 3(a), showing $\Delta_{\max}$ as a function of n, that for well widths $w = 15$ nm and barrier thickness $t_B = 10$ nm, the onset density $n_0 \sim 0.5 \times 10^{10}$ cm^{-2} is an order of magnitude smaller than for the optical measurements.

Since the lowest density attained in the drag experiments was $n \gtrsim 4 \times 10^{10} \gg n_0$, we conclude that the anomalous behavior reported in the drag experiments is most probably not an indication of a superfluid transition.

Figure 3(a) shows the onset density could be markedly increased to reach the minimum densities attained in Ref. [32] by relatively minor reductions in w and t_B. However, interface roughness scattering increases rapidly as the well is made narrower, resulting in samples with very low mobilities. Nevertheless, even if no macroscopically connected superfluid remained, superfluidity may well survive in pockets randomly distributed along the quantum wells. Such pockets of superfluidity could be detected using capacitance spectroscopy [51].

In capacitance spectroscopy, a low-frequency ac voltage is delivered to a top gate with the quantum wells grounded. The total capacitance $C_m = (C_g^{-1} + C_Q^{-1})^{-1}$ between the gate and the quantum wells is measured. C_g is the classical geometry capacitance per unit area which depends only on the sample structure. $C_Q = e^2\partial n/\partial\mu$ is the quantum capacitance and is proportional to the density of states. For a two-dimensional system in the normal state, $C_Q^N = (1/A)[e^2m^*/(\pi\hbar^2)]$,

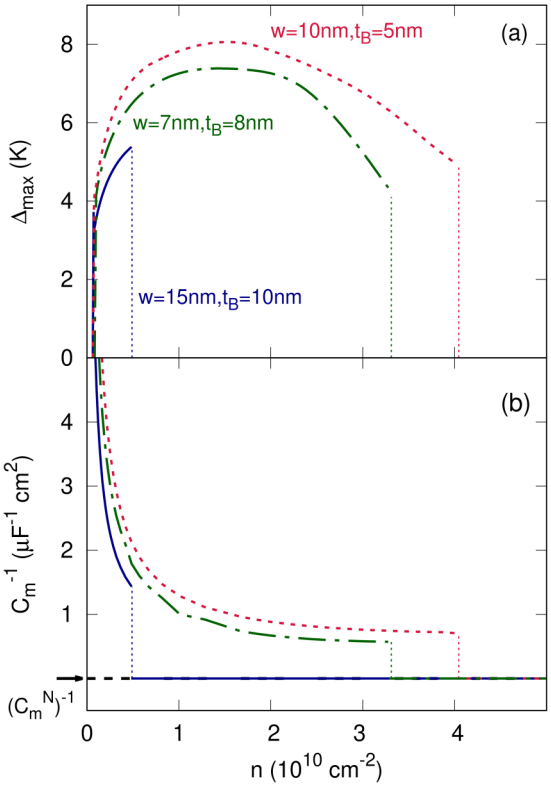

FIG. 3. (a) $\Delta_{\max}$ as a function of n. The solid blue line: $w = 15$ and $t_B = 10$ nm (sample: Ref. [32]); the dashed-dotted green line: $w = 7$ and $t_B = 8$ nm; the dotted red line: $w = 10$ and $t_B = 5$ nm. (b) Corresponding inverse of total capacitance C_m^{-1} as a function of density n. The inverse of total capacitance in the normal state $(C_m^N)^{-1}$ is indicated.

inversely proportional to the sample area. For a pocket of superfluidity of area $A' \leqslant A$, the quantum capacitance is as follows:

$$C_Q^S = \frac{1}{A'}\left[e^2 \sum_{\mathbf{k}} \delta(\mu - \epsilon_F) + 4e^2 \sum_{\mathbf{k}} \frac{u_{\mathbf{k}}^2 v_{\mathbf{k}}^2}{E_k}\right]. \quad (5)$$

$C_Q^S < C_Q^N$ because of the gap in the low-lying energy spectrum [51,52].

Figure 3(b) shows the inverse of the total capacitance C_m^{-1} as a function of density for homogeneous systems. From Fig. 3(a), the onset density for superfluidity for well widths $w = 10$ nm and barrier thickness $t_B = 5$ nm is $n_0 \sim 4 \times 10^{10}$ cm^{-2}. C_m^N is the corresponding total capacitance in the normal state. The onset of superfluidity is characterized by a jump in C_m^{-1} at n_0, and C_m^{-1} monotonically increases as the density is further decreased. For the inhomogeneous system with pockets of superfluid of total area A', the behavior would be similar, but the jump in C_m^{-1} at n_0 would be reduced by an amount proportional to (A'/A).

Table I shows the effects on the superfluid properties of band bending and the finite width of the quantum wells for samples from Ref. [32]. We saw, in Fig. 1, that band bending pushes the peaks of the electron and hole density distributions (d_p) further apart than the distance between the centers of the wells (d_c). The effect of this in weakening the superfluidity can be seen by comparing rows A and B. In row B, band bending has been neglected. The finite thickness of the wells also weakens the superfluidity. This can be seen by comparing row A with row C, calculated for the same d_c but neglecting the well widths. For a fixed distance between the centers of the wells d_c, narrower wells with a thicker barrier also weaken the superfluidity, a combined effect of banding bending and the gate potentials [35]. This is seen by comparing rows A and D. The ratio r_0/d_p, where r_0 is the average spacing of the electrons at the superfluid onset density n_0, is a useful indicator of the effect of the heterostructure parameters on n_0. The table shows that n_0 occurs for a value of the ratio $r_0/d_p \sim 2.5$–3. For smaller r_0, the screening is too strong, and the superfluidity cannot overcome the screening.

The unusually large effective mass difference between electrons and holes in GaAs makes experimental realization of superfluidity in GaAs double quantum wells a particularly worthwhile goal, likely to reveal intriguing new physics. Although, in principle, this physics can also be investigated with ultracold atoms of different masses, the exotic superfluid phases are predicted for the ultracold atom system only below nanokelvin temperatures, whereas, for GaAs, the transition temperatures are a few kelvins. The primary reason it has proved so difficult to observe superfluidity in GaAs is that the phenomenon only occurs at low densities due to strong screening at higher densities of the long-range Coulomb pairing interactions. Screening kills superfluidity above an onset density. To generate superfluidity in GaAs at accessible experimental densities requires narrow quantum wells and thin barriers that have been impractical for transport experiments because of the very low mobility of the samples. However, we show that inhomogeneous pockets of superfluidity could be detected in samples of low mobility using standard capacitance measurement techniques. Finally, our calculations confirm that superfluid condensation of optically generated

TABLE I. (A) Double quantum well structure from Ref. [32]; (B) same structure, calculated without band bending; (C) same structure, calculated for the same d_c but with the width of the quantum wells neglected; (D) A different double quantum well structure with the same d_c as (A). Columns: w is the quantum well widths, t_B is the barrier thickness, d_c is the distance between centers of the two wells, d_p is the distance between the peaks of the electron and hole density distributions, n_0 is the superfluid onset density with r_0 as the corresponding average interelectron spacing, $\bar{\Delta}$ is the maximum value of $\Delta_{\max}$ across all densities, and T^{BKT} is maximum superfluid transition temperature.

	w (nm)	t_b (nm)	d_c (nm)	d_p (nm)	n_0 (10^{10} cm^{-2})	r_0/d_p	$\bar{\Delta}$ (K)	T^{BKT} (K)
A	15	10	25	27	0.5	3.0	5.2	0.1
B	15	10	25	25	0.8	2.5	6.2	0.3
C	15	10	25	25	1.0	2.3	8.3	0.4
D	10	15	25	29	0.4	3.1	4.0	0.1

electron-hole pairs is, indeed, feasible with existing experimental samples.

We thank K. Das Gupta, F. Dubin, U. Siciliani de Cumis, M. Pini, and J. Waldie for illuminating discussions. This work was partially supported by the Flemish Science Foundation (FWO-Vl) and the Australian Government through the Australian Research Council Centre of Excellence in Future Low-Energy Electronics (Project No. CE170100039).

[1] M. Bartenstein, A. Altmeyer, S. Riedl, S. Jochim, C. Chin, J. H. Denschlag, and R. Grimm, Crossover From a Molecular Bose-Einstein Condensate to a Degenerate Fermi Gas, Phys. Rev. Lett. **92**, 120401 (2004).

[2] C. A. Regal, M. Greiner, and D. S. Jin, Observation of Resonance Condensation of Fermionic Atom Pairs, Phys. Rev. Lett. **92**, 040403 (2004).

[3] M. W. Zwierlein, C. A. Stan, C. H. Schunck, S. M. F. Raupach, A. J. Kerman, and W. Ketterle, Condensation of Pairs of Fermionic Atoms Near a Feshbach Resonance, Phys. Rev. Lett. **92**, 120403 (2004).

[4] A. Perali, D. Neilson, and A. R. Hamilton, High-Temperature Superfluidity in Double-Bilayer Graphene, Phys. Rev. Lett. **110**, 146803 (2013).

[5] S. Conti, M. Van der Donck, A. Perali, F. M. Peeters, and D. Neilson, A doping-dependent switch from one- to two-component superfluidity at temperature above 100K in coupled electron-hole Van der Waals heterostructures, arXiv:1909.03411.

[6] G. W. Burg, N. Prasad, K. Kim, T. Taniguchi, K. Watanabe, A. H. MacDonald, L. F. Register, and E. Tutuc, Strongly Enhanced Tunneling at Total Charge Neutrality in Double-Bilayer Graphene-WSe_2 Heterostructures, Phys. Rev. Lett. **120**, 177702 (2018).

[7] D. K. Efimkin, G. W. Burg, E. Tutuc, and A. H. MacDonald, Tunneling and fluctuating electron-hole Cooper pairs in double bilayer graphene, Phys. Rev. B **101**, 035413 (2020).

[8] Z. Wang, D. A. Rhodes, K. Watanabe, T. Taniguchi, J. C. Hone, J. Shan, and K. F. Mak, Evidence of high-temperature exciton condensation in two-dimensional atomic double layers, Nature (London) **574**, 76 (2019).

[9] A. Chaves and D. Neilson, Exotic state seen at high temperatures, Nature (London) **574**, 39 (2019).

[10] I. B. Spielman, J. P. Eisenstein, L. N. Pfeiffer, and K. W. West, Resonantly Enhanced Tunneling in a Double Layer Quantum Hall Ferromagnet, Phys. Rev. Lett. **84**, 5808 (2000).

[11] C. Comte and P. Nozières, Exciton Bose condensation : The ground state of an electron-hole gas - I. Mean field description of a simplified model, J. Phys. France **43**, 1069 (1982).

[12] L. V. Keldysh and Y. V. Kopaev, Possible instability of semimetallic state toward Coulomb interaction, Sov. Phys. Solid State USSR **6**, 2219 (1965).

[13] L. V. Keldysh and A. N. Kozlov, Collective properties of excitons in semiconductors, Sov. Phys. JETP **27**, 521 (1968).

[14] Y. E. Lozovik and V. I. Yudson, Feasibility of superfluidity of paired spatially separated electrons and holes, JETP Lett. (USSR) **22**, 274 (1975).

[15] Y. E. Lozovik and V. I. Yudson, A new mechanism for superconductivity: pairing between spatially separated electrons and holes, Zh. Eksp. Teor. Fiz **71**, 738 (1976) [Sov. Phys. JETP **44**, 389 (1976)].

[16] S. Conti, A. Perali, F. M. Peeters, and D. Neilson, Multicomponent screening and superfluidity in gapped electron-hole double bilayer graphene with realistic bands, Phys. Rev. B **99**, 144517 (2019).

[17] S. Saberi-Pouya, M. Zarenia, A. Perali, T. Vazifehshenas, and F. M. Peeters, High-temperature electron-hole superfluidity with strong anisotropic gaps in double phosphorene monolayers, Phys. Rev. B **97**, 174503 (2018).

[18] C. Ravensbergen, V. Corre, E. Soave, M. Kreyer, E. Kirilov, and R. Grimm, Production of a degenerate Fermi-Fermi mixture of dysprosium and potassium atoms, Phys. Rev. A **98**, 063624 (2018).

[19] P. Pieri, D. Neilson, and G. C. Strinati, Effects of density imbalance on the BCS-BEC crossover in semiconductor electron-hole bilayers, Phys. Rev. B **75**, 113301 (2007).

[20] J. J. Kinnunen, J. E. Baarsma, J.-P. Martikainen, and P. Törmä, The Fulde–Ferrell–Larkin–Ovchinnikov state for ultracold fermions in lattice and harmonic potentials: A review, Rep. Prog. Phys. **81**, 046401 (2018).

[21] B. Frank, J. Lang, and W. Zwerger, Universal phase diagram and scaling functions of imbalanced Fermi gases, J. Exp. Theor. Phys. **127**, 812 (2018).

[22] J. Wang, Y. Che, L. Zhang, and Q. Chen, Enhancement effect of mass imbalance on Fulde-Ferrell-Larkin-Ovchinnikov type of pairing in Fermi-Fermi mixtures of ultracold quantum gases, Sci. Rep. **7**, 39783 (2017).

[23] M. M. Forbes, E. Gubankova, W. V. Liu, and F. Wilczek, Stability Criteria for Breached-Pair Superfluidity, Phys. Rev. Lett. **94**, 017001 (2005).

[24] J. E. Baarsma and H. T. C. Stoof, Inhomogeneous superfluid phases in ^{6}Li - ^{40}K mixtures at unitarity, Phys. Rev. A **87**, 063612 (2013).

[25] Y-C. Zhang, F. Maucher, and T. Pohl, Supersolidity Around a Critical Point in Dipolar Bose-Einstein Condensates, Phys. Rev. Lett. **123**, 015301 (2019).

[26] D. Neilson, A. Perali, and A. R. Hamilton, Excitonic superfluidity and screening in electron-hole bilayer systems, Phys. Rev. B **89**, 060502(R) (2014).

[27] P. López Ríos, A. Perali, R. J. Needs, and D. Neilson, Evidence from Quantum Monte Carlo Simulations of Large-Gap Superfluidity and BCS-BEC Crossover in Double Electron-Hole Layers, Phys. Rev. Lett. **120**, 177701 (2018).

[28] L. V. Butov, A. C. Gossard, and D. S. Chemla, Macroscopically ordered state in an exciton system, Nature (London) **418**, 751 (2002).

[29] A. A. High, J. R. Leonard, M. Remeika, L. V. Butov, M. Hanson, and A. C. Gossard, Condensation of excitons in a trap, Nano Lett. **12**, 2605 (2012).

[30] R. Anankine, M. Beian, S. Dang, M. Alloing, E. Cambril, K. Merghem, C. G. Carbonell, A. Lemaître, and F. Dubin,

Quantized Vortices and Four-Component Superfluidity of Semiconductor Excitons, Phys. Rev. Lett. **118**, 127402 (2017).

[31] V. B. Timofeev and A. V. Gorbunov, Collective state of the Bose gas of interacting dipolar excitons, J. Appl. Phys. **101**, 081708 (2007).

[32] A. F. Croxall, K. Das Gupta, C. A. Nicoll, M. Thangaraj, H. E. Beere, I. Farrer, D. A. Ritchie, and M. Pepper, Anomalous Coulomb Drag in Electron-Hole Bilayers, Phys. Rev. Lett. **101**, 246801 (2008).

[33] J. A. Seamons, C. P. Morath, J. L. Reno, and M. P. Lilly, Coulomb Drag in the Exciton Regime in Electron-Hole Bilayers, Phys. Rev. Lett. **102**, 026804 (2009).

[34] G. Vignale and A. H. MacDonald, Drag in Paired Electron-Hole Layers, Phys. Rev. Lett. **76**, 2786 (1996).

[35] B. Zheng, A. F. Croxall, J. Waldie, K. Das Gupta, F. Sfigakis, I. Farrer, H. E. Beere, and D. A. Ritchie, Switching between attractive and repulsive Coulomb-interaction-mediated drag in an ambipolar GaAs/AlGaAs bilayer device, Appl. Phys. Lett. **108**, 062102 (2016).

[36] I. H. Tan, G. L. Snider, L. D. Chang, and E. L. Hu, A self-consistent solution of Schrödinger–Poisson equations using a nonuniform mesh, J. Appl. Phys. **68**, 4071 (1990).

[37] E. I Rashba, Properties of semiconductors with an extremum loop. I. Cyclotron and combinational resonance in a magnetic field perpendicular to the plane of the loop, Sov. Phys., Solid State **2**, 1109 (1960).

[38] See Supplemental Material at http://link.aps.org/supplemental/10.1103/PhysRevB.101.140501 for full expressions of $V^{\ell\ell'}_{\mathbf{k}-\mathbf{k}'}$, which includes Refs. [4,32,33,36,47].

[39] U. Sivan, P. M. Solomon, and H. Shtrikman, Coupled Electron-Hole Transport, Phys. Rev. Lett. **68**, 1196 (1992).

[40] K. Flensberg and B. Y.-K. Hu, Plasmon enhancement of Coulomb drag in double-quantum-well systems, Phys. Rev. B **52**, 14796 (1995).

[41] M. Iskin and C. A. R. Sá de Melo, Mixtures of ultracold fermions with unequal masses, Phys. Rev. A **76**, 013601 (2007).

[42] I. Sodemann, D. A. Pesin, and A. H. MacDonald, Interaction-enhanced coherence between two-dimensional Dirac layers, Phys. Rev. B **85**, 195136 (2012).

[43] Z. W. Gortel and L. Świerkowski, Superfluid ground state in electron-hole double layer systems, Surf. Sci. **361**, 146 (1996).

[44] R. Bistritzer, H. Min, J.-J. Su, and A. H. MacDonald, Comment on "Electron screening and excitonic condensation in double-layer graphene systems", arXiv:0810.0331v1.

[45] J. M. Kosterlitz and D. J. Thouless, Ordering, metastability and phase transitions in two-dimensional systems, J. Phys. C: Solid State **6**, 1181 (1973).

[46] S. S. Botelho and C. A. R. Sá de Melo, Vortex-Antivortex Lattice in Ultracold Fermionic Gases, Phys. Rev. Lett. **96**, 040404 (2006).

[47] Y. E. Lozovik, S. L. Ogarkov, and A. A. Sokolik, Condensation of electron-hole pairs in a two-layer graphene system: Correlation effects, Phys. Rev. B **86**, 045429 (2012).

[48] L. Salasnich, N. Manini, and A. Parola, Condensate fraction of a Fermi gas in the BCS-BEC crossover, Phys. Rev. A **72**, 023621 (2005).

[49] A. Guidini and A. Perali, Band-edge BCS–BEC crossover in a two-band superconductor: physical properties and detection parameters, Supercond. Sci. Technol. **27**, 124002 (2014).

[50] F. Pistolesi and G. C. Strinati, Evolution from BCS superconductivity to Bose condensation: Calculation of the zero-temperature phase coherence length, Phys. Rev. B **53**, 15168 (1996).

[51] L. Du, X. Li, W. Lou, G. Sullivan, K. Chang, J. Kono, and R-R. Du, Evidence for a topological excitonic insulator in InAs/GaSb bilayers, Nat. Commun. **8**, 1971 (2017).

[52] M. J. Yang, C. H. Yang, B. R. Bennett, and B. V. Shanabrook, Evidence of a Hybridization Gap in "Semimetallic" InAs/GaSb Systems, Phys. Rev. Lett. **78**, 4613 (1997).